# Production of Dense Plasmas with sub-10-fs Laser Pulses

J. Osterholz,[1] F. Brandl,[1] T. Fischer,[1] D. Hemmers,[1] M. Cerchez,[1] G. Pretzler,[1] O. Willi,[1] and S. J. Rose[2]

[1]*Institute of Laser and Plasmaphysics, Heinrich-Heine-University Düsseldorf, Germany*

[2]*Department of Physics, Clarendon Laboratory, University of Oxford, Oxford, United Kingdom*

(Received 17 June 2005; published 28 February 2006)

Close to solid state density plasmas with peak electron temperatures of about 190 eV have been generated with sub-10-fs laser pulses incident on solid targets. Extreme ultraviolet (XUV) spectroscopy is used to investigate the $K$ shell emission from the plasma. In the spectra, a series limit for the H- and He-like resonance lines becomes evident which is explained by pressure ionization in the dense plasma. The spectra are consistent with computer simulations calculating the XUV emission and the expansion of the plasma.

DOI: 10.1103/PhysRevLett.96.085002 PACS numbers: 52.38.Dx, 52.25.Os, 52.65.−y

The interaction of intense, subpicosecond laser pulses with solid targets allows the generation of dense plasmas with a temperature between 10 eV and 1 keV [1–8]. Matter under these conditions plays an important role in various fields of research such as astrophysics [9,10], inertial confinement fusion (ICF) [11], and the development of ultrafast x-ray sources. Plasmas generated with subpicosecond laser pulses are also an interesting tool to study the x-ray opacity of matter under conditions found in the interior of stars [12] and for the development of x-ray diagnostics used in ICF research [13]. In addition, they are used as a benchmark for kinetic computer simulations [14] and the investigation of the equation of state of matter under extreme conditions [15]. For this research, typically spectroscopy in the XUV and x-ray spectral range is used to determine the plasma conditions. For example the density is obtained from line broadening effects, the emission of satellites, or series limits of resonance lines. Besides XUV spectroscopy, other methods for the investigation of dense plasmas have been reported, e.g., in [16,17].

A prerequisite for the generation of dense plasmas is a fast, efficient transfer of the laser energy to the solid region of the target. Absorption experiments highlight the role of the preplasma scale length and the hydrodynamic expansion of the plasma during the interaction [18–21]. The scale length is typically larger than the electron skin depth and the expanding overcritical plasma does not allow for the penetration of the laser pulse to the solid region of the target. Instead the laser energy is absorbed close to the critical surface where the density is much smaller than solid. The production of dense plasmas under these conditions requires an efficient transfer of energy from the critical surface into the solid region of the target by thermal electrons. The hydrodynamic expansion of the heated region of the target during the interaction can be suppressed with tamped targets [1,2], although it still plays an important role in these experiments.

A different kind of energy transfer to the solid region of the target can be achieved if during the laser pulse the plasma scale length is smaller than the plasma electron skin depth. Under these conditions the evanescent field of the laser pulse penetrates into the solid region of the target. A fraction of the laser energy is absorbed by collisional heating in the skin layer [22,23]. In the past, however, the small preplasma scale length required for this kind of interaction could only be achieved in experiments with relatively small irradiances [e.g., $I < 5 \times 10^{12}$ W/cm$^2$ in [24] ].

Here we demonstrate the generation of dense plasmas with high-contrast sub-10-fs laser pulses with an intensity of $10^{16}$ W/cm$^2$ on solid targets. To our knowledge this is the first experimental investigation of the interaction of sub-10-fs laser pulses with dense plasmas. In the experiments time integrated XUV spectroscopy investigating the $K$ shell emission from the target was used to determine plasma density and temperature. In the spectra a series limit is observed which is explained by pressure ionization. The expansion and the XUV emission of the plasma are analyzed with computer simulations. In the simulations the laser is absorbed in the skin layer and the plasma is still close to solid density at the laser peak. The calculated XUV spectra are in good agreement with the experiment.

For the experiment a chirped pulse amplification laser system consisting of a Ti:sapphire oscillator and a Ti:sapphire multipass amplifier similar to that described in [25] was used. After compression in a prism compressor, laser pulses with a length of 30 fs (FWHM) and an energy of 700 $\mu$J at 1 kHz repetition rate were obtained. Further compression of the pulses was achieved with a second compressor consisting of an argon-filled hollow fiber and a set of specially designed chirped mirrors [26]. A pulse length of 8 fs was determined with a second order autocorrelator. Because of transmission losses by the second compressor and the mirrors in the beam line, the pulse energy on target was 200 $\mu$J. The laser beam was focussed with an $f/3$ off-axis parabola. The focal spot with 10 $\mu$m diameter contained 50% of the laser energy resulting in an average intensity in the focal region of $10^{16}$ W/cm$^2$. The pulse contrast (in intensity) was larger than $10^5$ for the time

 

larger than 1 ps and larger than $10^8$ for the time larger than 6 ps before the main pulse.

With a pulse energy of 200 $\mu$J the emission of the $K$ shell resonance lines can only be achieved with targets with a small atomic number. Therefore carbon (C) and boron nitride (BN) targets were used. For the low-$Z$ ions the $K$ shell emission is in the XUV spectral range. In the experiment XUV emission was investigated with a flat-field grazing incidence spectrograph in the spectral range between 1 and 20 nm [27]. Varied-spacing concave gratings (nominal spacing 1200 and 2400 lines/mm) were used in the spectrometer. The emitted XUV radiation was imaged onto the spectrometer entrance slit and the detector image plane, respectively, with two gold coated grazing incidence collector mirrors. An intensified x-ray CCD camera containing a phosphor scintillator with a 100 nm aluminum coating and a microchannel plate image amplifier was used as detector. The spectral resolution of the spectrometer achieved in this experiment was $\lambda/\Delta\lambda \approx 100$ at 5 nm.

The targets were solid, rectangular slabs with dimensions of $5 \times 5$ cm$^2$ (BN) and $2.5 \times 2.5$ cm$^2$ (C) and 2 mm in thickness. The $p$-polarized laser beam was incident onto the target at an angle of 45° with respect to the target normal. The XUV spectra were time integrated over a number of $2 \times 10^5$–$8 \times 10^5$ shots corresponding to a time between 200 and 800 s. During this time the target was moved laterally with a velocity of 250 $\mu$m/s keeping the target surface in the focal position.

A typical carbon spectrum is shown in Fig. 1 where the C VI $1s$-$2p$ (C Ly$_\alpha$, 3.37 nm) and the C V $1s^2$-$1s2p$ (C He$_\alpha$, 4.03 nm) lines are identified. The intensity of the C V $1s^2$-$1s3p$ (C He$_\beta$, 3.50 nm) line is only slightly above the noise level for the sub-10-fs pulses. A boron nitride spectrum is shown in Fig. 2. In this spectrum the N VII $1s$-$2p$ (N Ly$_\alpha$, 2.48 nm), N VI $1s^2$-$1s2p$ (N He$_\alpha$, 2.88 nm), B V $1s$-$2p$ (B Ly$_\alpha$, 4.86 nm), B IV $1s^2$-$1s2p$ (B He$_\alpha$, 6.03 nm), and B IV $1s^2$-$1s3p$ (B He$_\beta$, 5.27 nm) lines are identified. It is noted that there might also be a contribution from the N VI $1s^2$-$1s3p$ (N He$_\beta$, 2.49 nm), as the N Ly$_\alpha$ and N He$_\beta$ lines cannot be resolved with the spectrometer. It is evident that there is no significant contribution from the C VI $1s$-$3p$ (C Ly$_\beta$, 2.85 nm) and the B V $1s$-$3p$ (B Ly$_\beta$, 4.10 nm) lines in the spectra.

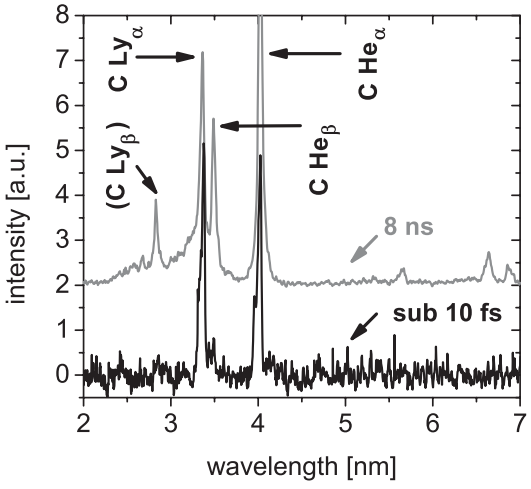


FIG. 1. XUV spectra obtained from C targets. For the sub-10-fs laser pulses, the C Ly$_\beta$ and higher lines are suppressed by pressure ionization. In contrast they are clearly visible in the spectrum obtained with 8 ns pulses (plotted with an offset).

XUV spectra obtained with longer laser pulses typically contain the higher series lines. This has been confirmed in two additional experiments. In the first experiment a frequency doubled Nd:YAG laser with 8 ns, 120 mJ pulses, resulting in a focus intensity of $5 \times 10^{12}$ W/cm$^2$, was used in the same experimental setup. In the carbon spectrum in Fig. 1 measured with this laser the Ly and He series including recombination emission are clearly visible. In the second experiment the pulses of the Ti:sapphire system were stretched to a length of 200 fs. In this experiment a significant contribution of the Ly$_\beta$ lines was observed. The lack of the higher lines in the sub-10-fs spectra indicates that the plasma is at high density where pressure ionization has removed the upper levels [6,7]. We analyzed the effect of pressure ionization for the targets used in this experiment with the IMP code [28]. IMP calculates the potential around an ion in the plasma using the high-temperature Thomas-Fermi model. For this potential the Schrödinger equation is solved for different orbitals. In this way we determine which orbitals are and which orbitals are not allowed in the plasma. For a temperature of 100 eV (expected 300 fs after the laser peak, see below) the range of densities which allow for the emission of the Ly$_\alpha$ and suppress the Ly$_\beta$ lines is between $\rho_{\min} = 0.3$ g/cm$^3$ and $\rho_{\max} = 0.8$ g/cm$^3$ for BN and between $\rho_{\min} = 0.2$ g/cm$^3$ and $\rho_{\max} = 1.3$ g/cm$^3$ for C.

For a more detailed analysis the XUV emission was calculated with time dependent FLY simulations [29]. A computer model was developed to calculate the basic

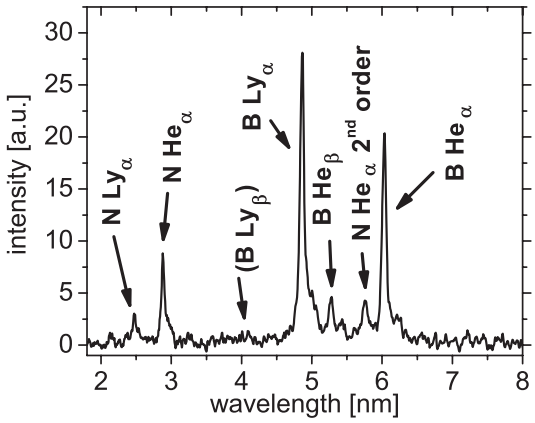


FIG. 2. XUV spectrum obtained from a BN target. The B Ly$_\beta$ and higher lines are suppressed by pressure ionization.

plasma parameters as input for the atomic physics calculations. In this model it is assumed that a fraction $f_{\mathrm{th}}$ of the laser energy is deposited in a layer with an initial thickness of $\delta_0 = 10$ nm corresponding to the electron skin depth, and is converted into thermal energy of the plasma. The absorbing layer is initially at solid density ($\rho_0 = 2.0\ \mathrm{g/cm^3}$ for BN, $2.25\ \mathrm{g/cm^3}$ for C). The layer with thickness $\delta(t)$ expands with the ion sound speed $c_S(t)$. Taking into account an adiabatic equation of state, we obtain for the plasma temperature $T(t)$ and the layer thickness $\delta(t)$:

$$\frac{d}{dt}kT(t) = \frac{2}{3}\frac{f_{\mathrm{th}}P_L(t)}{N} - (\gamma - 1)\frac{c_S(t)}{\delta(t)}kT(t) \qquad (1)$$

$$\frac{d}{dt}\delta(t) = c_S(t) = \sqrt{(Z + \gamma)kT(t)/M}, \qquad (2)$$

where $k$ is the Boltzmann constant, $N$ is the total number of particles (free electrons and ions) in the heated plasma volume, $P_L(t)$ is the incident laser power, $\gamma = 5/3$ is the adiabatic exponent, and $M$ is the average ion mass. The first term on the right side of Eq. (1) takes into account the energy transfer from the laser to the plasma, whereas the second term represents cooling of the plasma during the adiabatic expansion. The ion sound speed $c_S(t)$ is calculated assuming an average ion charge $Z = 4.5$ (for both the BN and the C target) and the same temperature for electrons and ions [30]. The plasma density $\rho$ is obtained from $\rho(t) = \rho_0 \cdot \delta_0/\delta(t)$ taking into account that the expansion can be considered one dimensional as long as the focal diameter is larger than the emitting plasma layer thickness. Equations (1) and (2) were solved numerically with the temporal evolution of the laser power $P_L(t)$ determined from the Fourier transform of the laser spectrum. As the fraction of absorbed laser energy was not measured in the experiment, the calculations were carried out for different values of $f_{\mathrm{th}}$. The temporal evolution of the plasma temperature and density calculated for the BN target and $f_{\mathrm{th}} = 25\%$ are shown in Fig. 3. The peak of the pulse is at $t = 0$. For this value of $f_{\mathrm{th}}$ the electron temperature increases rapidly to a peak value of about $T_p = 190$ eV. At this time, the plasma density is about 80% of solid. In the subsequent expansion phase, plasma temperature and density decrease with a time constant of the order of 1 picosecond.

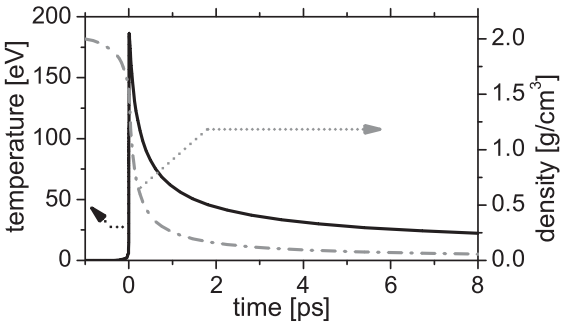


FIG. 3. Expansion of the BN plasma layer calculated with a numerical model. Left axis: temperature; right axis: density.

The XUV emission from the expanding plasma was then calculated with time dependent FLY simulations [29]. Line broadening including Stark and Doppler broadening, and opacity effects were taken into account. For the analysis of the experiment, we calculated the intensity ratios of the $\mathrm{Ly}_\alpha/\mathrm{He}_\alpha$ lines from the time integrated spectra. The result is shown in Fig. 4 for $T_p = 150$ eV, 190 eV, and 220 eV (corresponding to $f_{\mathrm{th}} = 20\%$, 25%, and 30% for BN, respectively). In addition, the line intensity ratios obtained in the experiment are plotted in Fig. 4. The measured data agree well with the calculations for a value of $T_p = 190$ eV, whereas it significantly differs from the synthetic spectra for $T_p = 150$ eV and $T_p = 220$ eV. From the errors of the intensity ratios a temperature variation of 20% is possible. For all lines the optical depth is smaller than 1 at the time of the maximum emitted intensity, except for the N $\mathrm{He}_\alpha$ for which the optical depth is 1.2.

The expansion model yields a preplasma scale length $l = 2.4$ nm which is smaller than the initial electron skin depth $\delta_0 = 10$ nm. This indicates that the energy is transferred from the laser pulse to the dense region of the target by skin layer absorption. The calculations predict a rise time of the temperature from 6 eV to its maximum of about 190 eV in less than 20 fs. During this time, the plasma layer thickness increases only about 6%. This result demonstrates that the energy transfer can be considered as instantaneous on the hydrodynamic time scale for the sub-10-fs laser pulse. In contrast, the model predicts for longer laser pulses significantly larger plasma layer thicknesses (e.g., 40 nm at the peak temperature for a 100 fs FWHM Gaussian pulse with the same peak intensity) and consequently it is expected that the interaction is not anymore dominated by skin layer absorption.

In the time dependent FLY simulations, the plasma is initially at high density and the $\mathrm{Ly}_\beta$ and $\mathrm{He}_\beta$ and higher

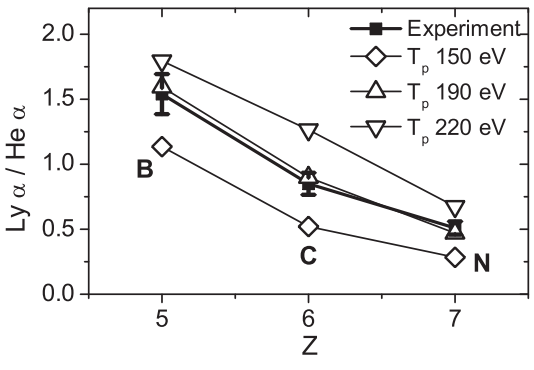


FIG. 4. Intensity ratios of the $\mathrm{Ly}_\alpha/\mathrm{He}_\alpha$ resonance lines observed in the experiment and calculated with time dependent FLY simulations for different peak temperatures $T_p$.

lines are suppressed by pressure ionization for all elements (B, C, and N). At a later stage of the expansion the density becomes smaller and the higher lines are emitted, too. However, their contribution to the XUV emission is very small. This is attributed to the rapid cooling of the plasma after the laser pulse. In the synthetic time integrated spectra, the ratio of the peak intensities of the $Ly_\beta/Ly_\alpha$ and $He_\beta/He_\alpha$ lines is smaller than 0.041 and 0.086, respectively. The calculated intensity of the $Ly_\beta$, $He_\gamma$, and higher lines is below the noise level of the measured spectra, and consequently they are not observed in the experiment. However, the contribution from the B $He_\beta$ line measured in the experiment is larger than in the FLY simulations. This might indicate that the expansion model is less precise at later times ($>10$ ps after the laser peak) when heat conduction, which is not included in the model, becomes important. The effect of pressure ionization in the expanding plasma was also analyzed with the IMP code. In these calculations the onset of the higher lines is at later times than predicted by FLY, and consequently one would expect yet smaller contributions from the higher series lines to the time integrated spectra.

It is noted that conditions close to local thermodynamic equilibrium (LTE) in highly transient, dense plasmas have been reported in [31]. This issue was investigated with a second set of FLY simulations calculating the LTE populations for the expanding plasma. For the period up to about 100–200 fs after the laser peak, the time dependent populations significantly differ from LTE, but after this time they are close to the LTE populations. According to [32], LTE requires an electron density which satisfies

$$n_e\ [\mathrm{cm}^{-3}] \geq 1.6 \times 10^{12} \sqrt{T_e\ [\mathrm{eV}]} (\Delta E_{\mathrm{Max}}\ [\mathrm{eV}])^3, \quad (3)$$

where $\Delta E_{\mathrm{Max}}$ is the energy difference between the ground state and the largest existing level of the considered ion species ($\approx$500 eV in our case). This condition is fulfilled demonstrating that the plasma is dominated by collisional processes. For example, the mean electron-ion collision time is $\tau_{ei} = 0.3$ fs, 300 fs after the laser peak. At this time the electron mean free path is $\lambda_{ei} = 1.8$ nm, which is more than 1 order of magnitude smaller than the emitting plasma layer thickness.

In summary, we have generated close to solid state density plasmas with a peak temperature of about 190 eV using 200 $\mu$J, sub-10-fs laser pulses with a high pulse contrast. Time integrated XUV spectroscopy is applied to derive the plasma conditions. In the spectra, a series limit is observed, demonstrating that dense plasmas are produced. The lack of the higher lines indicates that (i) there is no significant contribution from the preplasma to the XUV emission, (ii) that there is no significant expansion of the plasma during the laser pulse, and (iii) that the expansion after the laser pulse is accompanied by rapid cooling of the plasma. These issues are confirmed by the expansion model and the time dependent FLY simulations. The calculations indicate that the laser pulse is absorbed in a small layer with a thickness in the order of the plasma skin depth in the solid density region of the target. We conclude that few-cycle pulses allow the investigation of laser-plasma interaction in a novel regime.

This work has been performed within the SFB/Transregio TR 18 and GRK 1203. S. J. R. thanks AWE Aldermaston for support.

[1] A. Saemann *et al.*, Phys. Rev. Lett. **82**, 4843 (1999).
[2] K. Eidmann *et al.*, J. Quant. Spectrosc. Radiat. Transfer **81**, 133 (2003).
[3] U. Teubner *et al.*, Appl. Phys. B **62**, 213 (1996).
[4] J. C. Gauthier *et al.*, Phys. Plasmas **4**, 1811 (1997).
[5] J. C. Gauthier, in *Atoms, Solids and Plasmas in Super-Intense Laser Fields*, edited by D. Batani *et al.* (Kluwer Academic/Plenum Publishers, New York, 2001).
[6] M. Nantel *et al.*, Phys. Rev. Lett. **80**, 4442 (1998).
[7] A. Maksimchuk *et al.*, J. Quant. Spectrosc. Radiat. Transfer **65**, 367 (2000).
[8] D. Riley *et al.*, Phys. Rev. Lett. **69**, 3739 (1992).
[9] D. D. Ryutov and B. A. Remington, Plasma Phys. Controlled Fusion **44**, B407 (2002).
[10] S. Ichimaru, Rev. Mod. Phys. **54**, 1017 (1982).
[11] J. D. Lindl *et al.*, Phys. Plasmas **11**, 339 (2004).
[12] N. Nazir *et al.*, Appl. Phys. Lett. **69**, 3686 (1996).
[13] N. C. Woolsey *et al.*, Phys. Rev. E **57**, 4650 (1998).
[14] R. W. Lee *et al.*, J. Quant. Spectrosc. Radiat. Transfer **58**, 737 (1997).
[15] R. M. More, *Laser Interactions with Atoms, Solids and Plasmas* (Plenum, New York, 1994).
[16] D. Giulietti *et al.*, Phys. Rev. Lett. **79**, 3194 (1997).
[17] S. Dobosz *et al.*, Phys. Rev. Lett. **95**, 025001 (2005).
[18] W. Rozmus *et al.*, Phys. Plasmas **3**, 360 (1996).
[19] M. Borghesi *et al.*, Phys. Rev. E **60**, 7374 (1999).
[20] D. F. Price *et al.*, Phys. Rev. Lett. **75**, 252 (1995).
[21] R. Sauerbrey *et al.*, Phys. Plasmas **1**, 1635 (1994).
[22] W. Rozmus and V. T. Tikhonchuk, Phys. Rev. A **42**, 7401 (1990).
[23] W. Rozmus and V. T. Tikhonchuk, Phys. Rev. A **46**, 7810 (1992).
[24] J. C. Kieffer *et al.*, Phys. Rev. Lett. **62**, 760 (1989).
[25] M. Hentschel *et al.*, Appl. Phys. B **70**, 161 (2000).
[26] Z. Cheng *et al.*, Opt. Lett. **24**, 247 (1999).
[27] A. Saemann and K. Eidmann, Rev. Sci. Instrum. **69**, 1949 (1998).
[28] S. J. Rose, J. Phys. B **25**, 1667 (1992).
[29] R. W. Lee and J. T. Larsen, J. Quant. Spectrosc. Radiat. Transfer **56**, 535 (1996).
[30] W. L. Kruer, *The Physics of Laser Plasma Interactions* (Addison-Wesley, Reading, MA, 1988).
[31] P. Audebert *et al.*, Phys. Rev. Lett. **94**, 025004 (2005).
[32] R. W. P. McWhirter, in *Plasma Diagnostic Techniques*, edited by R. H. Huddlestone and S. L. Leonard (Academic, New York, 1965).